Journal of Cellular Biochemistry 68:511–524 (1998)

Metabolites of the Phospholipase D Pathway Regulate H_2O_2-Induced Filamin Redistribution in Endothelial Cells

Laurie E. Hastie,[1] Wayne F. Patton,[1] Herbert B. Hechtman,[2] and David Shepro[1]*

[1]Microvascular Research Laboratory, Biological Sciences and Photonics Center, Boston University, Boston, Massachusetts 02215
[2]Department of Surgery, Harvard Medical School, Boston, Massachusetts 02115

Abstract Hypoxia/reoxygenation injury to cultured endothelial cells results in cytoskeletal rearrangement and second messenger activation related to increased monolayer junctional permeability. Cytoskeletal rearrangement by reactive oxygen species may be related to specific activation of the phospholipase D (PLD) pathway. Human umbilical vein endothelial cell monolayers are exposed to H_2O_2 (100 μM) or metabolites of the PLD pathway for 1–60 min. Changes in cAMP levels, Ca^{2+} levels, PIP_2 production, filamin distribution, and intercellular gap formation are then quantitated. H_2O_2-induced filamin translocation from the membrane to the cytosol occurs after 1-min H_2O_2 treatment, while intercellular gap formation significantly increases after 15 min. H_2O_2 and phosphatidic acid exposure rapidly decrease intracellular cAMP levels, while increasing PIP_2 levels in a Ca^{2+}-independent manner. H_2O_2-induced cAMP decreases are prevented by inhibiting phospholipase D. H_2O_2-induced cytoskeletal changes are prevented by inhibiting phospholipase D, phosphatidylinositol-4-phosphate kinase, phosphoinositide turnover, or by adding a synthetic peptide that binds PIP_2. These data indicate that metabolites produced downstream of H_2O_2-induced PLD activation may mediate filamin redistribution and F-actin rearrangement. J. Cell. Biochem. 68:511–524, 1998.

Key words: actin; permeability; reoxygenation; signal transduction; cytoskeletal rearrangement

Endothelial cells (EC) of microvessels provide a barrier between blood and tissues. When this barrier is breached, a major percentage of fluid and protein passes through the EC intercellular junctions to the tissues [Dejana et al., 1995; Goldman et al., 1991; Patton et al., 1991]. Ischemia/reperfusion (I/R) injury is known to cause an increase in the number and diameter of EC junctional gaps [Welbourn et al., 1991; Wiles et al., 1993]. EC are exposed to H_2O_2 from activated neutrophils and from the dismutation of superoxide in EC that follows hypoxia/reoxygenation injury. The resulting effect from such exposure is disassembly of the dense peripheral band (DPB) of F-actin and intercellular gap formation [Liu and Sundqvist, 1995]. The signal transduction mechanism leading to this cytoskeletal response is unknown.

EC monolayers, exposed to inflammatory agonists such as thrombin or bradykinin, are characterized by a loss of the DPB and increased stress fiber formation, which is thought to increase paracellular gap formation [Lum and Malik, 1994]. Rearrangement of other cytoskeletal proteins also occurs prior to, or simultaneous with, actin rearrangement. We have previously evaluated the membrane-cytoskeletal actin binding protein nonmuscle filamin (ABP-280) in EC oxidative injury [Hastie et al., 1997a]. EC filamin redistributes from the membrane to the cytosol following H_2O_2 exposure, in a Ca^{2+}-independent and cAMP-dependent manner [Hastie et al., 1997a,b]. The translocation of filamin from the membrane to the cytosol occurs immediately prior to actin rearrangement; thus, it may trigger disassembly of the DPB of actin that leads to a decrease of close EC junc-

Contract grant sponsor: National Institutes of Health; Contract grant numbers: HL-43875, HL-48553, GM-24891, GM-35141.

Dr. Laurie Hastie's current address is Dept. of Pathology, Brigham and Women's Hospital, Boston, MA 02115.

Dr. Wayne Patton's current address is Molecular Probes, Inc., Eugene, OR, 97402.

*Correspondence to: David Shepro, Microvascular Research Laboratory, Boston University, 5 Cummington Street, Boston, MA 02215.

Received 15 September 1997; Accepted 20 October 1997

tional apposition. H_2O_2-induced filamin redistribution and DPB disassembly are prevented by antioxidants or elevated cAMP levels [Hastie et al., 1997a,b].

EC exposure to H_2O_2 activates phopholipase D (PLD) [Kiss and Anderson, 1994; Natarajan et al., 1993], which results in the hydrolysis of phosphatidylcholine and increased phosphatidic acid formation [Shasby et al., 1988; Natarajan et al., 1993, 1996]. Phosphatidic acid may be a potent second messenger in oxidative injury, since it has been shown to: increase actin polymerization [Cross et al., 1996], decrease adenylate cyclase activity [Murayama and Ui, 1987], increase cAMP phosphodiesterase activity [Marcoz et al., 1993], activate ras protein [Tsai et al., 1989, 1990], increase phosphatidylinositol-4-phosphate (PIP) kinase activity [Moritz et al., 1992]. Indeed, H_2O_2 appears to increase PIP_2 formation [Shasby et al., 1988], possibly through activation of PIP kinase. Interestingly, filamin is a potent actin cross-linker that upon exposure to phosphatidylinositol 4,5-biphosphate (PIP_2) dissociates from actin [Furuhashi et al., 1992; Janmey, 1994]. The effects of PLD metabolites on EC cytoskeletal changes during oxidative injury are largely unknown.

This study demonstrates that H_2O_2-induced EC filamin translocation and junctional gap formation may be regulated in part by increased levels of phosphatidic acid and PIP_2. We have previously shown that H_2O_2-induced filamin translocation and intercellular gap formation are cAMP-dependent [Hastie et al., 1997b]. The H_2O_2-induced cytoskeletal changes may result from phosphatidic acid generation and PIP_2 production, in addition to decreased cAMP levels. Our data suggest that intracellular PIP_2 levels influence filamin distribution, possibly by binding to filamin. Pharmacological agents that prevent PLD activation and PIP_2 formation also inhibit H_2O_2-induced filamin translocation and intercellular gap formation.

MATERIALS AND METHODS

Materials

Reagents were obtained as follows: butylated hydroxytoluene, phosphatidic acid, and 3-isobutyl-1-methylxanthine (IBMX) from Sigma (St. Louis, MO), hydroxynonenal, propranolol, and LY294002 from Biomol (Plymouth Meeting, PA), wortmannin, SQ22536, genistein, and neomycin sulfate from LC Laboratories (Woburn, MA), phosphatidylinositol 4,5-bisphosphate from Calbiochem (La Jolla, CA), and H_2O_2 from Fisher (Pittsburgh, PA). Myristoylated peptides (NH_2-GWAPECAPLKSKM-COOH) and (NH_2-TGPR-LVSNHSLHE-COOH) are synthesized by Quality Control Biochemicals (Hopkinton, MA).

Methods

Endothelial cell isolation and cultivation. Human umbilical vein endothelial cells (HUVEC) are isolated and propagated by an adaptation of previously described methods [Shepro et al., 1974]. HUVEC are used between passages 1 to 4 and are maintained in endothelial basal medium (Clonetics, San Diego, CA) supplemented with 10% fetal bovine serum (FBS), 1.0 µg/ml hydrocortisone, 100 U/ml penicillin, 100 µg/ml streptomycin, 0.25 µg/ml amphotericin, and 20 µg/ml endothelial growth supplement. Cells are fed every 2–3 days, subcultured by trypsinization, and reseeded in a 1:3 split ratio.

Preparation of subcellular fractions. Cellular proteins are fractionated into cytosol, membrane-organelle, nuclear, and cytoskeleton fractions as previously described [Ramsby et al., 1994; Hastie et al., 1997a; Wang et al., 1996]. Briefly, HUVEC seeded onto 100-mm dishes are rinsed twice in PBS (Ca^{2+} and Mg^{2+} free) and extracted in ice-cold digitonin buffer (0.01% digitonin, 10 mM PIPES, pH 6.8, 300 mM sucrose, 100 mM NaCl, 5 mM EDTA, 3 mM $MgCl_2$, protease inhibitors) on ice for 10 min while shaking at 50 rpm. The supernatant (cytosol fraction) is collected and ice-cold Triton X-100 buffer (0.5% Triton X-100, 10 mM PIPES, pH 7.4, 300 mM sucrose, 100 mM NaCl, 3 mM EDTA, 3 mM $MgCl_2$, protease inhibitors) is added to the residual cell fraction on ice for 30 min while shaking at 50 rpm. The supernatant (membrane-organelle fraction) is collected and ice-cold Tween-40/deoxycholate buffer (10 mM PIPES, 1% Tween-40, 0.5% deoxycholate, pH 7.4, 10 mM NaCl, 1 mM $MgCl_2$, protease inhibitors) is added on ice for 10 min while shaking at 50 rpm. The supernatant (nuclear-associated fraction) is collected and 100°C sample buffer I (10 mM Tris–HCl, pH 8.0, 2.5% SDS, 30 mg/ml DTT protease inhibitors) is added for 2–3 min, the cell fraction is scraped, sample buffer II (10 mM Tris–HCl, pH 8.0, 1 mg/ml DNase I, 0.25 mg/ml RNase I, 50 mM $MgCl_2$, protease inhibitors) is added and cellular proteins are incubated on ice for 5–6 min. The supernatant (cytoskeletal fraction) is collected; all samples are

acetone-precipitated and normalized to volume by redissolving in 100 µl sample buffer I.

Immunoblotting and filamin quantitation. Quantification of filamin content in each of the four fractions is as follows: cell extracts, dissolved in 100-µl sample buffer, are subjected to sodium dodecyl sulfate–polyacrylamide gel electrophoresis (SDS–PAGE) using 4–15% gradient gels (Pharmacia, NJ) according to the manufacturer's protocol. Equal volume of each fraction is loaded on gels. After electrophoresis, proteins are electroblotted for 1 h to 0.4-µm pore size nitrocellulose membrane (BioRad, CA) using the Pharmacia Phast system [Towbin et al., 1979]. Alternatively, cytosol and membrane/organelle fractions are solubilized in 100-µl sample buffer I and applied to nitrocellulose membranes using a BioRad slot-blot apparatus (Hercules, CA).

Nitrocellulose membranes from either electroblotting or slot blotting are blocked in 5% (BSA) (Sigma), 0.1% Tween-20 solution for 1 h, then incubated overnight at room temperature in 1:250 dilution of mouse antihuman nonmuscle filamin monoclonal antibody (Chemicon, Temecula, CA). Membranes are washed 3 × 15 min with wash buffer and incubated at room temperature for 1 h in a 1:2,000 dilution of alkaline phosphatase-conjugated goat antimouse IgG antibody (Cappel, Durham, NC, USA). Membranes are washed 3 × 15 min and bands are visualized using an alkaline phosphatase chromogenic buffer (100 mM tris-HCl, 100 mM NaCl, 5 mM $MgCl_2$, pH 9.5) containing 0.34 mg/ml nitroblue tetrazolium/0.17 mg/ml 5-bromo-4-chloro-3-indoylphosphate p-toluidine (Sigma) for 10 min in the dark. Blots are scanned at 300 dots per inch (dpi) resolution with 256 gray scale levels using a flat bed scanner interfaced to an Apple Macintosh Power PC microcomputer. Protein is quantified using NIH image, a public domain graphics program developed by Dr. W. Rasband, Research Services Branch, NIMH (wayne@helix.nih.gov).

Analysis of intercellular gaps. HUVEC are grown to confluence on gelatin coated glass coverslips. After exposure to various agents, cells are fixed in 1% glutaraldehyde-formalin buffer for 10 min. Cells are washed with phosphatase-buffered saline (PBS), Ca^{2+} and Mg^{2+}-free, and permeabilized in 0.2% Triton X-100 for 15 min. After washing, cells are stained with 10 mM rhodamine-phalloidin (Sigma) for 30 min in the dark. Coverslips are washed, mounted onto microscope slides with glycerol–H_2O (9:1), and viewed under an inverted IM-35 Zeiss fluorescent microscope. Cells are photographed using an Olympus OM-25 camera attachment and Kodak Tri-X Pan film at 40× objective. Negatives are scanned at 150 dots per inch (dpi) resolution with 256 gray scale levels using a flat bed scanner interfaced to an Apple Macintosh Power PC microcomputer. Gaps are quantified using NIH image.

Measurement of cAMP

The effects of selected agonists on intracellular cAMP levels in HUVEC are quantified by radioimmunoassay (cAMP kit; DuPont, New England Nuclear, Boston, MA). HUVEC are grown to confluence on 6-well plates and used in experiments at two days post-confluence. Cells are treated with either Hank's balanced salt solution (HBSS) alone or the appropriate agonist in HBSS. The reactions are terminated by washing the cells twice in ice-cold HBSS, and the protein is extracted using 6% trichloroacetic acid (TCA). The wells are scraped using a rubber policeman, and samples are sonicated at 4°C. The amount of protein per well is quantified using the BCA protein assay (Pierce, Rockford, IL). To extract cAMP, TCA extracts are centrifuged at 12,000*g* for 6 min. The supernatant is collected and extracted 4× with 5× volume of water-saturated ether to remove the TCA. The ether phase is discarded and the sample is evaporated to dryness under a stream of air. The dried sample is reconstituted in sodium acetate buffer at the appropriate dilution so as to be in the midpoint of the standard curve (determined in previous experiments). To determine the recovery of cAMP during extraction, a tritiated cyclic nucleotide marker is added to the sample after scraping. cAMP recovery is found to be 95%.

Intracellular calcium measurement. EC are seeded onto glass coverslips and allowed to grow to confluency. Cells are incubated in media containing 8 µM Fura-2/AM for 30 min at 37°C. They are washed three times with physiological saline solution containing 150 mM NaCl, 5 mM KCl, 1.8 mM $CaCl_2$, 5 mM glucose, 1 mM $MgCl_2$, 10 mM HEPES, pH 7.4. The coverslip is transferred into a cell holder and placed into a quartz cuvette. Fluorescence is measured using a Perkin-Elmer LS-50 spectrofluorometer (Perkin-Elmer, Buckinghamshire, England). A water bath is used to maintain the

temperature at 37°C. The cells are allowed to equilibrate in the cuvette for 10 min. The excitation wavelength alternates between 340 nm and 380 nm with the emission wavelength fixed at 510 nm. For calibration, 10 μM ionomycin is added, followed by the addition of 5 mM EGTA. The intracellular free Ca^{2+} is calculated from the ratio of the 340/380 nm-induced emission at 510 nm.

Phosphatidylinositol 4,5-bisphosphate (PIP_2) analysis. EC in 60-mm-diameter tissue culture plates are incubated with 1.1×10^7 cpm ^{3}H-inositol for 24–48 h, washed once, and then exposed to 100 μM H_2O_2 or 100 μM phosphatidic acid in HBSS for 1–10 min. The buffer is removed, and the cells are scraped following the addition of 2 ml ice-cold methanol. The lipids are extracted by the subsequent addition of 2 ml methanol, 2 ml chloroform, 1.4 ml 2.4 N HCl, 2 ml chloroform, and 2 ml 2.4 N HCl. The phases are separated by centrifugation at 2,000*g* for 10 min. The lower chloroform phase is washed with methanol:2.4 N HCl, dried under nitrogen, and redissolved in a mixture of 2-propanol, ammonia, and water (55:15:35). Cold PIP_2 (1 mg/ml) is added to each sample, samples are spotted on silica gel plates (Merck, Darmstadt, Germany), and lipids are separated using thin layer chromatography in a buffer solvent containing 2-propanol, ammonia, and water (55:15:35). PIP_2 standard is visualized with iodine vapor, and radioactivity of each sample comigrating with PIP_2 is quantified by liquid scintillation counting.

Modulation of cytoskeletal changes by a synthetic peptide. A synthetic peptide corresponding to a site on the actin binding protein cofilin that binds PIP_2 (PIP_2 peptide) is synthesized by Quality Control Biochemicals (Hopkinton, MA). The peptide is based on the deduced amino acid sequence of cofilin that has been shown to bind PIP_2 [Yonezawa et al., 1991]. The peptide contains amino acid residues 103-115 of cofilin (NH_2-GWAPECAPLKSKM-COOH). A control peptide, corresponding to amino acid residues 2517–2529 of nonmuscle filamin, is synthesized by the same company. The control peptide has the amino acid sequence of NH_2-TGPRLVSNHSLHE-COOH and corresponds to filamin's C-terminal calcium/calmodulin protein kinase II phosphorylation site (CaM peptide). Since the selected regions correspond to internal fragments of actin binding proteins, an N-terminal acetyl and C-terminal amide are included in the synthetic peptide sequences. Cell permeability is achieved by addition of myristyl moieties to the N-termini of the peptides. Peptide purity is confirmed by reverse-phase HPLC and laser desorption mass spectrometry. Greater than 99% of each peptide eluted as a single peak upon analysis by reverse-phase HPLC. The m/z ratio of the two peptides are found by mass spectrometry to be 1,625 Da and 1,665 Da, respectively.

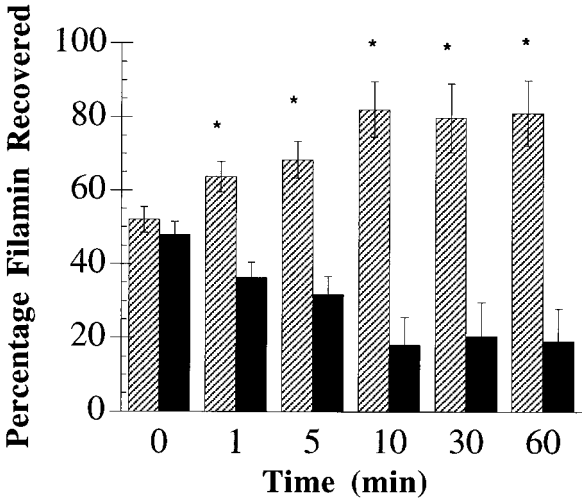

Fig. 1. Time course of H_2O_2-induced filamin translocation. Cells are exposed to 100 μM H_2O_2 for the indicated times. Filamin distribution: black bars, membrane fraction; hatched bars, cytosol fraction. H_2O_2-induced translocation is compared with controls (untreated cells): $^{**}P < 0.01$. Error bars = means ±SD (n = 3).

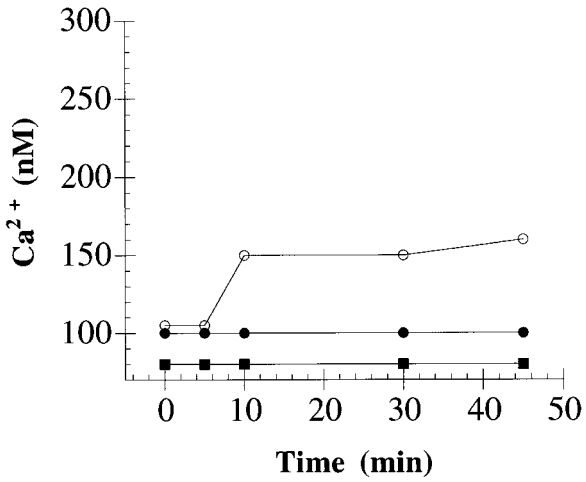

Fig. 2. Agonist induced changes in intracellular Ca^{2+}. Representative tracings show changes in intracellular Ca^{2+} levels in HUVEC treated with the indicated concentrations of agonist. Treatments are as follows: closed circles, control, open circles, 100 μM phosphatidic acid; closed squares, 50 μM PIP_2.

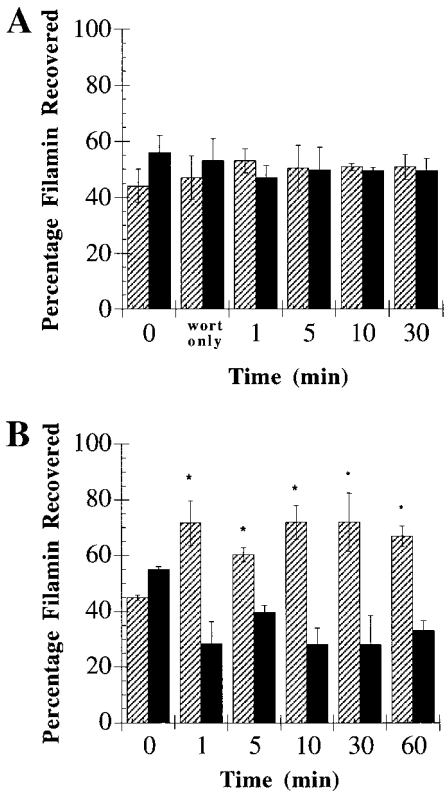

Fig. 3. Regulation of H_2O_2-induced filamin translocation by metabolites of the phospholipase D pathway. Wortmannin mediated protection from H_2O_2-induced filamin translocation and phosphatidic acid induced filamin translocation. **A:** Filamin distribution in cells pretreated with 5 μM wortmannin for 30 min prior to H_2O_2 (100 μM) exposure for 1–30 min. **B:** Filamin distribution in cells treated with phosphatidic acid (100 μM) for 1–60 min. Black bars, membrane fraction; hatched bars, cytosol fraction. There is no significant difference in translocation between wortmannin-treated cells and controls. Phosphatidic acid-treated cells are compared with controls (untreated cells): $*P <$ 0.05. Error bars = means ±SD (n = 3 for each group).

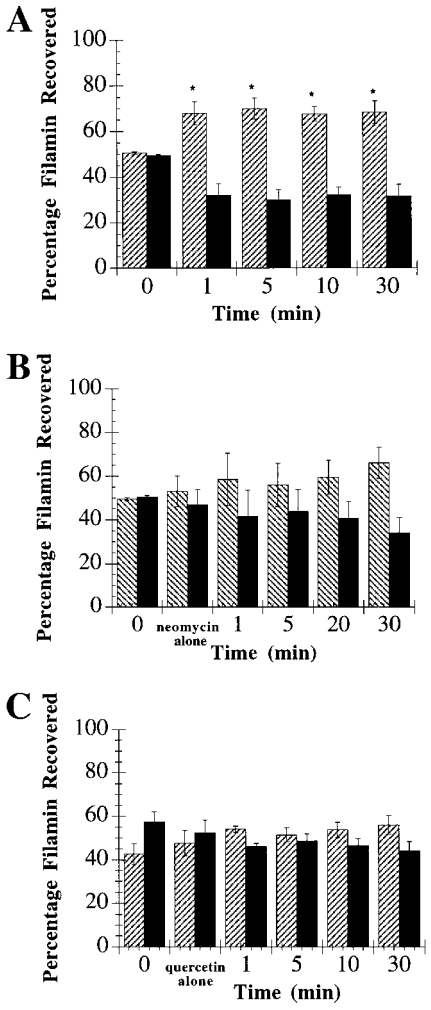

Fig. 4. Regulation of H_2O_2-induced filamin translocation by phosphoinositide activity. **A:** Filamin distribution in cells treated with PIP_2 (50 μM) for 1–30 min. **B:** Filamin distribution in cells pretreated with neomycin (50 μM) for 10 min prior to H_2O_2 (100 μM) exposure for 1–30 min. **C:** Filamin distribution in cells pretreated with quercetin (10 μM) for 10 min prior to H_2O_2 for 1–30 min. Black bars, membrane fraction; hatched bars, cytosol fraction. PIP_2 induces significant filamin translocation: $*P <$ 0.05. Pretreated cells inhibit H_2O_2-induced filamin translocation and are compared with controls (untreated cells): $*P <$ 0.02. Error bars = means ±SD (n = 3 for each group).

Statistics. Quantified parameters in treated cells are compared with values from untreated cells. In addition, HUVEC pretreated with various agonists prior to H_2O_2 treatment are compared with H_2O_2-treated cells. Results are expressed as means ±SD of 3 to 10 determinations. Differences in two groups are considered statistically significant when $P < 0.05$, using Welch's t-test.

RESULTS

Filamin Distribution in Endothelial Cells

We have shown previously that subcellular fractionation of EC using the differential detergent fractionation technique yields filamin primarily distributed among three compartments (35% in the membrane/organelle, 36% in the cytosol, and 23% in the cytoskeleton) with a small amount recovered (2–8%) in the nuclear fraction [Hastie et al., 1997a]. Upon exposure to 100 μM H_2O_2, filamin translocation from the membrane/organelle fraction to the cytosol fraction is observed at 1 min (Fig. 1). Translocation increases through 60 min with substantial translocation evident after 10 min. Filamin content in the cytoskeleton fraction and the nuclear fraction are unaltered by H_2O_2 exposure [Hastie et al., 1997a]. EC filamin is detected as a single 250-kD band prior to and after exposure

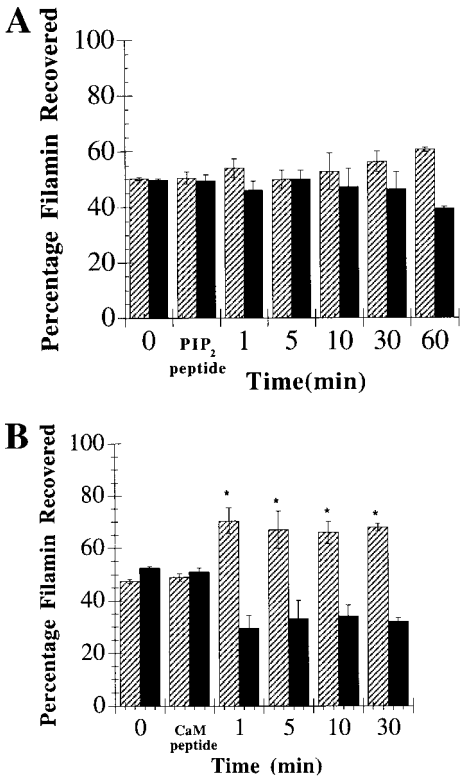

Fig. 5. Intracellular PIP_2 production in HUVEC exposed to **(A)** H_2O_2 (100 μM) for 1–10 min, or **(B)** phosphatidic acid (100 μM) for 1–10 min. Treated cells are compared with controls: $*P <$ 0.05. Error bars = means ±SD (n = 3 for each group).

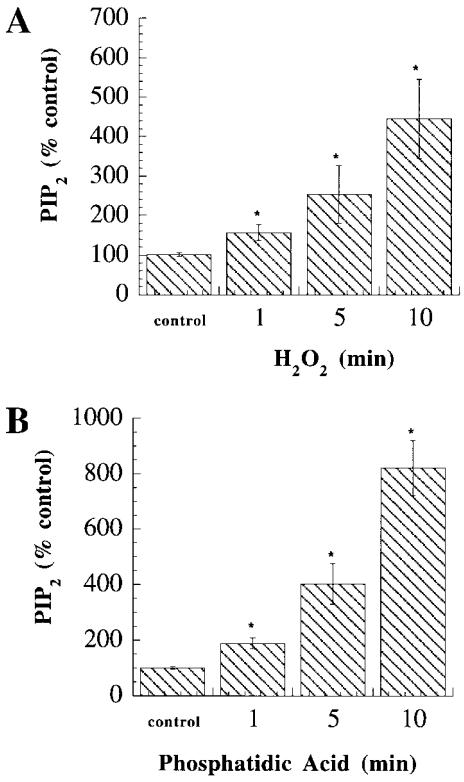

Fig. 6. Regulation of filamin translocation by a cell permeable peptide corresponding to a site on cofilin that binds PIP_2 (PIP_2 peptide). **A:** Filamin distribution in cells pretreated with PIP_2 peptide (10 μM) for 30 min prior to H_2O_2 (100 μM) for 1–30 min. **B:** Filamin distribution in cells pretreated with control peptide (10 μM) for 30 min prior to H_2O_2 (100 μM) for 1–30 min. Black bars, membrane fraction; hatched bars, cytosol fraction. Peptide-treated cells are compared with control (untreated cells): $*P < 0.02$. Error bars = means ±SD (n = 3 for each group).

to H_2O_2, which indicates that proteolysis of filamin does not occur [Hastie et al., 1997b].

Intracellular Calcium Levels

We have reported that exposing HUVEC to low levels of H_2O_2 (100 μM) does not increase intracellular Ca^{2+} levels above baseline (100 nM) through 30 min, which indicates that filamin translocation is not preceeded by an increase in Ca^{2+} [Hastie et al., 1997a]. Exogenous phosphatidic acid (100 μM) increases intracellular calcium to 150 nM after 10 min, with no further increases observed through 45 min (Fig. 2). PIP_2 (50 μM) does not increase intracellular calcium levels through 45 min (Fig. 2). These data indicate that phosphatidic acid initiated events prior to 10 min and PIP_2 initiated events prior to 45 min are Ca^{2+} independent.

Role of Phospholipase D Metabolites in Filamin Translocation

Inhibition of phospholipase D (PLD) by wortmannin pretreatment [Burstein et al., 1994; Naccache et al., 1993] for 30 min prevents H_2O_2-induced filamin translocation through 60 min (Fig. 3A). Since wortmannin is known to inhibit phosphatidyl inositol-3-kinase (PI-3-kinase), as well as PLD, EC are also pretreated with LY294002, a specific inhibitor of PI-3-kinase. Filamin translocation is not prevented by this agent (data not shown). To investigate further the role that phospholipase D activation plays in filamin translocation, EC are treated with 100 μM phosphatidic acid and found to undergo filamin translocation within 1 min (Fig. 3B). This translocation remains evident through 60 min. In vivo, phosphatidic acid is metabolized to diacylglycerol by the enzyme phosphatidate phosphohydrolase. If PLD-induced diacylglycerol is the initiator of filamin translocation, then inhibition of phosphatidate phosphohydrolase should prevent filamin movement. We de-

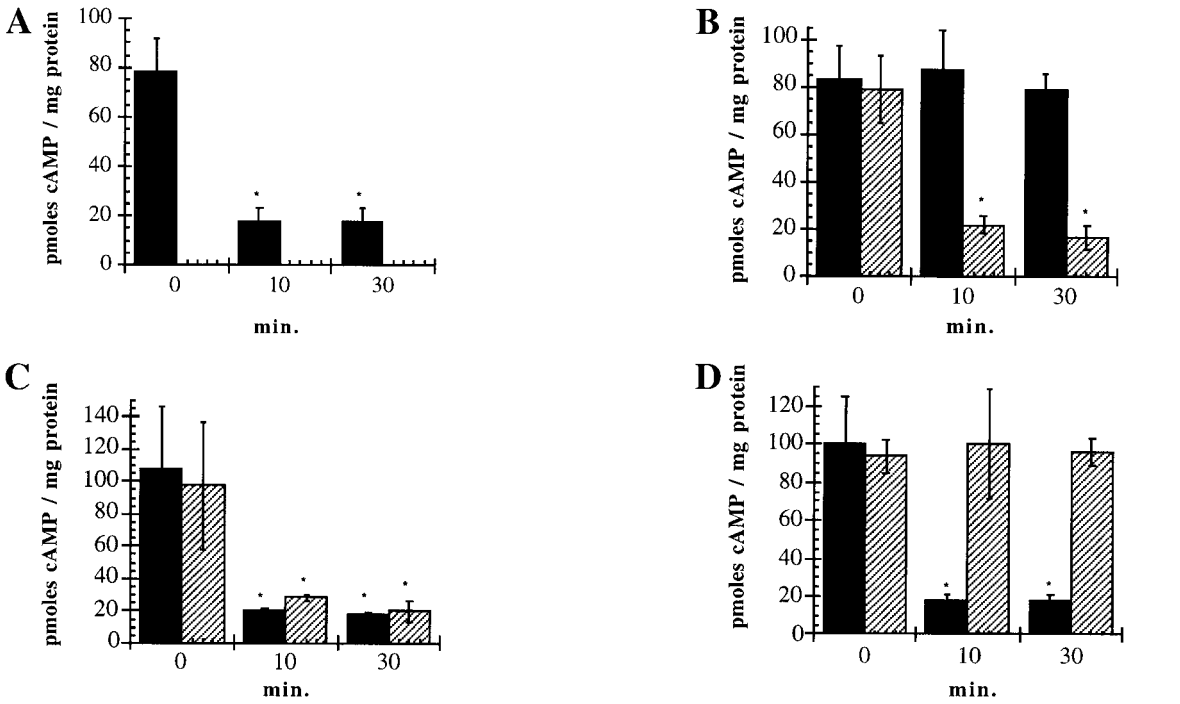

Fig. 7. cAMP levels. **A:** EC exposed to H_2O_2 (100 μM) for 10 and 30 min (black bars). **B:** Wortmannin (5 μM) pretreatment for 30 min prior to H_2O_2 exposure for 10 and 30 min (black bars); and phosphatidic acid (100 μM) for 10 and 30 min (hatched bars). **C:** Neomycin (50 μM) pretreatment for 10 min prior to H_2O_2 (100 μM) exposure for 10 and 30 min (black bars); and quercetin (10 μM) pretreatment for 10 min prior to H_2O_2 for 10 and 30 min (hatched bars). **D:** PIP_2 peptide (10 μM) pretreatment for 30 min prior to H_2O_2 (100 μM) for 10 and 30 min (black bars); and PIP_2 (50 μM) for 10 and 30 min (hatched bars). There is a significant decrease in cAMP levels in H_2O_2, phosphatidic acid, quercetin, and neomycin-treated cells compared with controls: $^*P < 0.01$. There is no significant difference in cAMP levels in wortmannin and PIP_2 treated cells compared with controls. Error bars = means ±SD (n = 3–5 for each group).

termined that phosphatidate phosphohydrolase inhibition, using propranolol, does not prevent filamin redistribution (data not shown).

Role of Phosphoinositides in Filamin Translocation

Filamin distribution is monitored in cells treated with agents that effect PIP_2 levels. Monolayer treatment with PIP_2 alone significantly induces filamin translocation within 1 min (Fig. 4A). Neomycin is known to specifically bind PIP_2 and inhibits its activity [Carney et al., 1985; Gabev et al., 1989]. Pretreatment with neomycin (50 μM) for 10 min delays H_2O_2-induced filamin translocation through 20 min (Fig. 4B). Quercetin inhibits 1-phosphatidylinositol 4-phosphate 5-kinase (PIP kinase) and 1-phosphatidylinositol 4-kinase (PI kinase) activity [Yeh et al., 1995]. Pretreatment with quercetin (10 μM) for 10 min, inhibits H_2O_2-induced filamin translocation through 30 min (Fig. 4C).

A synthetic peptide corresponding to a site on the actin binding protein cofilin that binds PIP_2 (PIP_2 peptide), is evaluated for its ability to inhibit filamin translocation. Pretreatment with PIP_2 peptide prior to H_2O_2 exposure (100 μM), significantly inhibits filamin translocation through 30 min. (Fig. 5A). This suggests that the PIP_2 peptide effectively competes with filamin for binding to cellular PIP_2. The same amount of a control peptide (CaM peptide) corresponding to filamin's C-terminal calcium/calmodulin protein kinase II phosphorylation site does not prevent H_2O_2-induced filamin translocation. (Fig. 5B).

Effects of H_2O_2 and Phosphatidic acid on Cellular PIP_2 Levels

H_2O_2 increases phosphatidic acid [Shasby et al., 1988; Natarajan et al., 1993, 1996] and PIP_2 levels in EC [Shasby et al., 1988]. Phosphatidic acid (PA) increases PIP kinase activity [Moritz

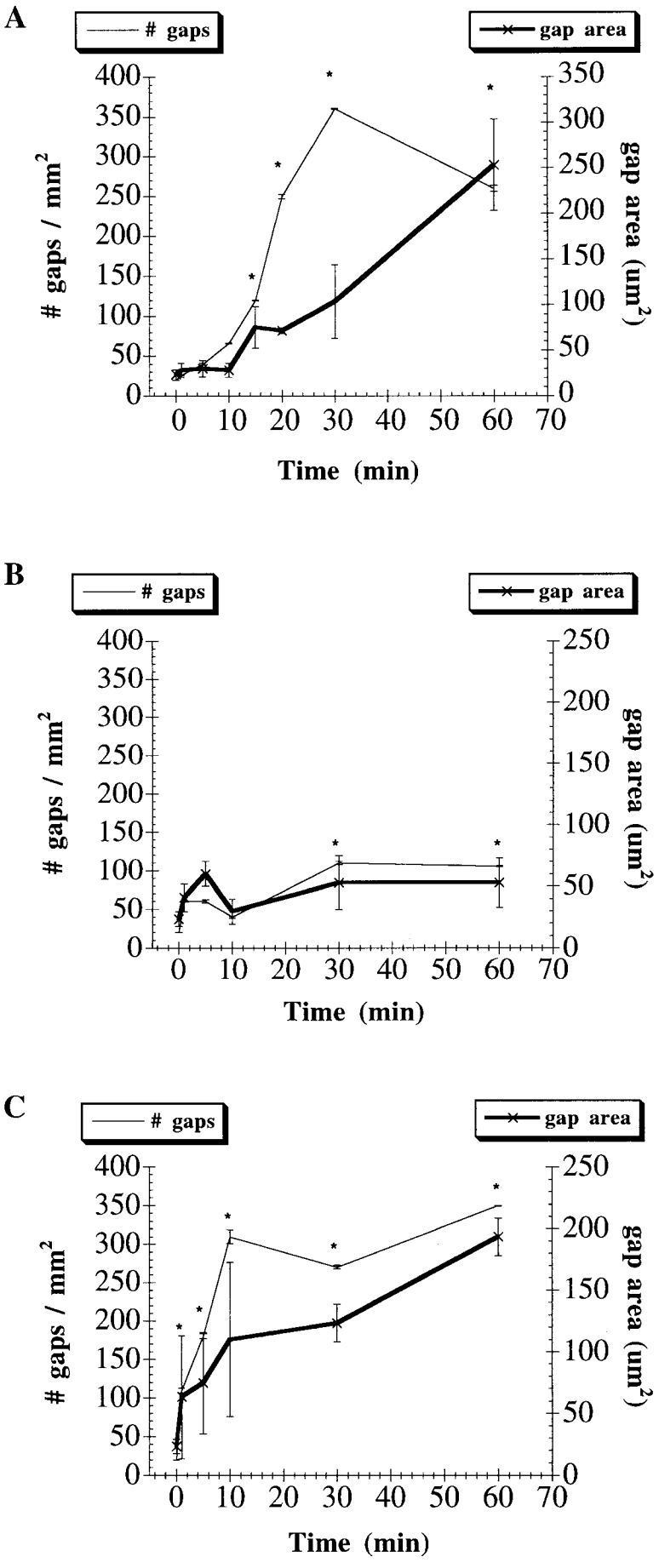
A
gaps
gap area
gaps / mm²
gap area (um²)
Time (min)
B
gaps
gap area
gaps / mm²
gap area (um²)
Time (min)
C
gaps
gap area
gaps / mm²
gap area (um²)
Time (min)

Figure 8.

et al., 1992], which should also result in increased PIP_2 formation. Since phosphoinositide hydrolysis influences filamin distribution, PIP_2 production is measured in HUVEC after exposure to H_2O_2 (100 μM) and phosphatidic acid (100 μM). One minute exposure to H_2O_2 significantly increases PIP_2 levels 57% above control (Fig. 6A). Five and 10 min exposures increase PIP_2 levels 153% and 344% above control, respectively. PA treatment significantly increases PIP_2 levels to 88%, 302%, and 720% above control at 1, 5, and 10 min, respectively (Fig. 6B).

cAMP Measurements

Changes in intracellular levels of cAMP are examined over a 30-min period after exposure to the indicated agonists. Baseline levels of cAMP in control cells is approximately 83 pmoles cAMP/mg protein (Fig. 7A). This decreases almost 5-fold after 1 min exposure to H_2O_2 and remains at low levels through at least 30 min H_2O_2 exposure (Fig. 7A). HUVEC pretreatment with wortmannin (5 μM) prior to exposure to H_2O_2 (100 μM) prevents decreases in intracellular cAMP levels and sustains levels at about 80 pmoles/mg protein (Fig. 7B). Exposure to phosphatidic acid (100 μM), a metabolite of phospholipase D activation, decreases intracellular cAMP levels 4-fold below baseline (Fig. 7B). Pretreatment with neomycin (50 μM) (Fig. 7C), quercetin (10 μM) (Fig. 7C), and PIP_2-peptide (10 μM) (Fig. 7D) prior to H_2O_2 does not prevent H_2O_2-induced cAMP decreases. Furthermore, exposure of EC to PIP_2 does not effect intracellular cAMP levels (Fig. 7D).

Role of Phospholipase D Metabolites in Intercellular Gap Formation

Upon exposure to H_2O_2, the number of intercellular gaps in cultured EC increases from baseline levels of 20 gaps/mm^2 to 120 gaps/mm^2 at 15 min (Fig. 8A). This steadily increases to approximately 360 gaps at 30 min, and decreases to 260 gaps at 60 min, presumably due to fusion of adjacent gaps. Average gap area remains at baseline levels through 10 min, then increases from 23 μm^2 to 75 μm^2 at 15 min. Average gap area remains at this level through 20 min, increases to 103 μm^2 at 30 min, and to 253 μm^2 at 60 min.

Wortmannin pretreatment inhibits the formation of intercellular gaps, with the gap number remaining below 120 gaps/mm^2 through 30- to 60-min exposure to H_2O_2, a 3-fold decrease compared to H_2O_2 alone (Fig. 8B). Average gap area remains below 60 μm^2; a 4-fold decrease compared to H_2O_2 alone.

Phosphatidic acid treatment induces gap formation in 1 min; at 10 min, there are 310 gaps/mm^2 (Fig. 8C). This number increases slightly to 350 gaps after 60 min. Average gap area likewise increases at 1 min to 63 μm^2 and steadily increases to a gap area of 193 μm^2 after 60 min.

Fig. 8. Quantification of intercellular gaps induced by H_2O_2 and phosphatidic acid, and prevented by wortmannin pretreatment. Thin line depicts no. of gaps/mm^2. Heavy line depicts average gap area (μm^2). **A:** EC stimulated with H_2O_2 for 1–60 min. **B:** EC pretreated with 5 μM wortmannin for 30 min prior to H_2O_2 for 1–60 min. **C:** EC treated with 100 μM phosphatidic acid for 1–60 min. Phosphatidic acid treated cells are compared with controls (untreated cells): $*P < 0.01$. Wortmannin-pretreated cells are compared with H_2O_2 treated cells: $*P < 0.02$. Error bars = means ±SD (n = 3 for each group).

Role of Phosphoinositides in Intercellular Gap Formation

Cell monolayers are treated with 50 μM PIP_2, and intercellular gaps are found to increase significantly from baseline after 30–60 min (Fig. 9A). Compared to H_2O_2 treated monolayers, there is a significant decrease in the number of gaps and average gap area from 20–60 min with neomycin pretreatment (Fig. 9B). Compared to H_2O_2 treated monolayers, there is a significant decrease in the number of gaps from 20–60 min with quercetin treatment (Fig. 9C).

Cells are pretreated with 10 μM PIP_2-peptide prior to H_2O_2 exposure. H_2O_2-induced intercellular gap formation is attenuated with PIP_2-peptide pretreatment (Fig. 10A). There is a significant decrease in the number of gaps at 20–60 min, when comparing PIP_2-peptide pretreated cells with H_2O_2 alone. At 20 and 30 min, the number of gaps is decreased 3-fold with PIP_2-peptide pretreatment. Average gap area also decreases 3-fold at 45 min with PIP_2-peptide pretreatment. An equivalent amount of the control, CaM peptide, does not inhibit H_2O_2-induced intercellular gap formation (Fig. 10B).

DISCUSSION

Recent evidence suggests that low concentrations of ROS activate second messenger pathways. ROS may increase vascular permeability through specific second messenger pathways

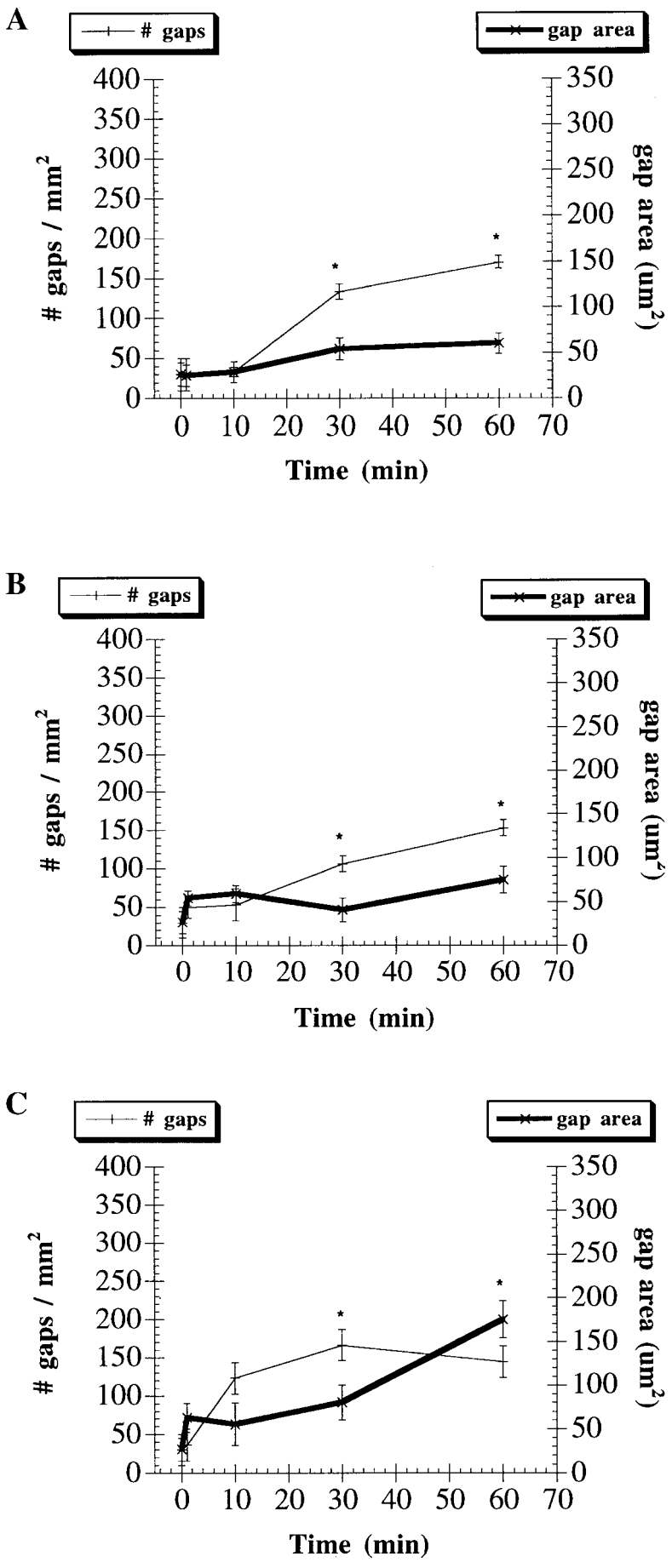
A
gaps
gap area
gaps / mm2
gap area (um2)
Time (min)
B
gaps
gap area
gaps / mm2
gap area (um2)
Time (min)
C
gaps
gap area
gaps / mm2
gap area (um2)
Time (min)

Figure 9.

rather than by nonspecific free radical attack. We report that filamin redistribution is an acute (within 1 min) response to H_2O_2 (100 μM) exposure in HUVEC [Hastie et al., 1997a]. Filamin translocation occurs prior to intercellular gap formation and increases in intracellular Ca^{2+}. Inhibition of the cAMP-dependent protein kinase pathway leads to decreases in filamin phosphorylation, which prevents H_2O_2-induced filamin redistribution [Hastie et al., 1997b].

H_2O_2 activates such mediators as phospholipase A, C, D, and protein kinase C [Shasby et al., 1988; Johnson et al., 1989; Natarajan et al., 1993]. We report that 100 μM H_2O_2 does not increase intracellular Ca^{2+} through 30 min in HUVEC [Hastie et al., 1997a]. These data indicate that a mediator dependent on intracellular Ca^{2+} for its activity, such as phospholipase A, or one that induces intracellular Ca^{2+} increases, such as phospholipase C, may not be involved in H_2O_2-induced filamin translocation. Natarajan and colleagues [1993] demonstrate that PLD activation in H_2O_2-exposed EC is independent of protein kinase C activation or intracellular calcium levels. The exact mechanism by which H_2O_2 activates phospholipase D is unknown.

Our data suggest that H_2O_2 activates phospholipase D, since the PLD inhibitor wortmannin prevents H_2O_2-mediated filamin translocation and paracellular gap formation. Phosphatidic acid, a metabolite of PLD activation, decreases adenylate cyclase activity, and activates phophodiesterases and PIP kinase [Amsterdam et al., 1994; van Corven et al., 1989; Murayama and Ui, 1987; Marcoz et al., 1993; Moritz et al., 1992]. We find in EC that phosphatidic acid decreases cAMP, increases PIP_2, and induces filamin translocation. H_2O_2 may decrease cAMP levels in EC by causing ATP depletion [Varani et al., 1990; Spragg et al., 1985]. Alternatively, cAMP levels may decrease, in part due to phosphatidic acid inhibition of adenylate cyclase and activation of phosphodiesterases.

H_2O_2 increases intracellular PIP_2 formation [Shasby et al., 1988]. The present study suggests that this may occur through phosphatidic acid-induced PIP kinase activity. Interestingly, PIP_2 binds to filamin and causes filamin to disassociate from actin [Furuhashi et al., 1992]. We find that exogenous PIP_2 induces filamin redistribution and intercellular gap formation, whereas inhibition of phosphoinositide activity attenuates H_2O_2-induced filamin translocation and gap formation. In addition, treating EC with a peptide that preferentially binds PIP_2, attenuates H_2O_2-induced filamin translocation and intercellular gap formation. We propose that H_2O_2 activates EC PLD, which increases intracellular phosphatidic acid. Phosphatidic acid in turn decreases cAMP levels and increases PIP_2 levels. PIP_2 may then bind filamin and induce its translocation from the membrane to the cytosol.

It is evident from this study that filamin distribution is regulated not only by cAMP levels [Hastie et al., 1997b], but by PIP_2 levels as well. Exogenous PIP_2 does not decrease cAMP levels, but filamin still translocates from the membrane to the cytosol. In addition, inhibition of phosphoinositide activity prevents H_2O_2-induced filamin translocation, even in the presence of decreased cAMP. This suggests that H_2O_2-induced PIP_2 increase, possibly through activation of PLD, induces filamin redistribution from the membrane to the cytosol.

It is a well documented observation that inflammatory agonists induce actin reorganization, but less evidence exists that explains the role of associated actin binding proteins. Filamin appears to be a key protein in EC cytoskeletal reorganization leading to permeability changes in the monolayer, since it redistributes prior to actin redistribution. H_2O_2 (100 μM)-treated EC induce filamin translocation in 1 min and intercellular gap formation in 10–15 min. We have previously shown that H_2O_2-induced filamin redistribution is accompanied by decreased cAMP levels, which leads to decreased phosphorylation of filamin at its cAMP-dependent protein kinase site. Not only does H_2O_2 decrease cAMP [Hastie et al., 1997b], but it also increases PIP_2 levels. We present evidence in this study that inhibition of H_2O_2-induced PIP_2 activity attenuates filamin trans-

Fig. 9. Quantification of H_2O_2-induced intercellular gaps modified by phosphoinositide activity. Thin line depicts no. of gaps/mm^2. Heavy line depicts average gap area (μm^2). **A:** EC stimulated with PIP_2 for 1–60 min. **B:** EC pretreated with 50 μM neomycin for 10 min prior to H_2O_2 for 1–30 min. **C:** EC pretreated with 10 μM quercetin for 1–30 min. PIP2 treated cells are compared with controls (untreated cells): $^*P < 0.01$. Pretreated cells are compared with H_2O_2-treated cells: $^*P < 0.05$. Error bars = means ±SD (n = 3 for each group).

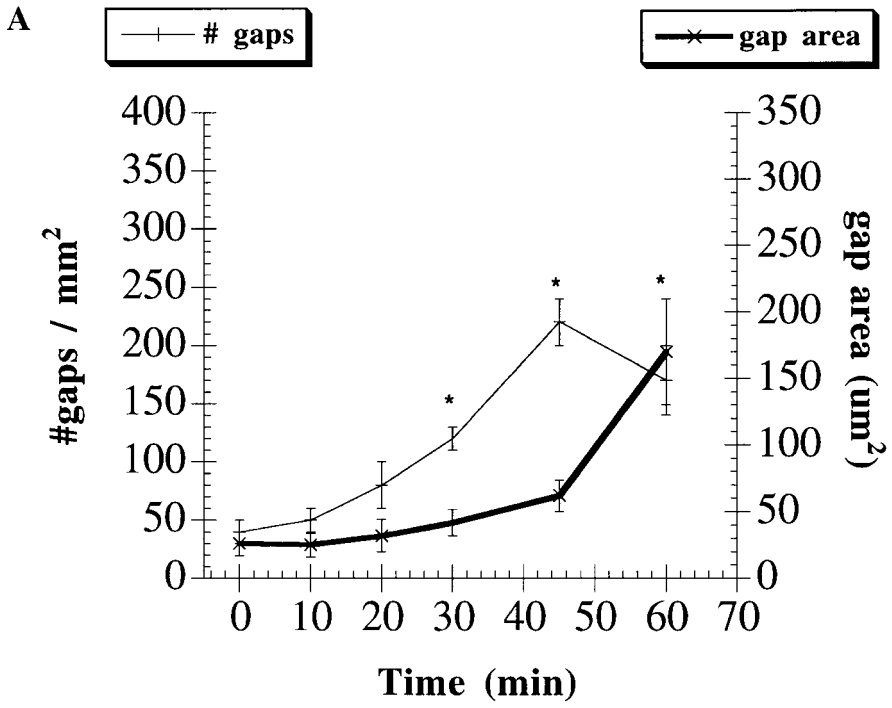

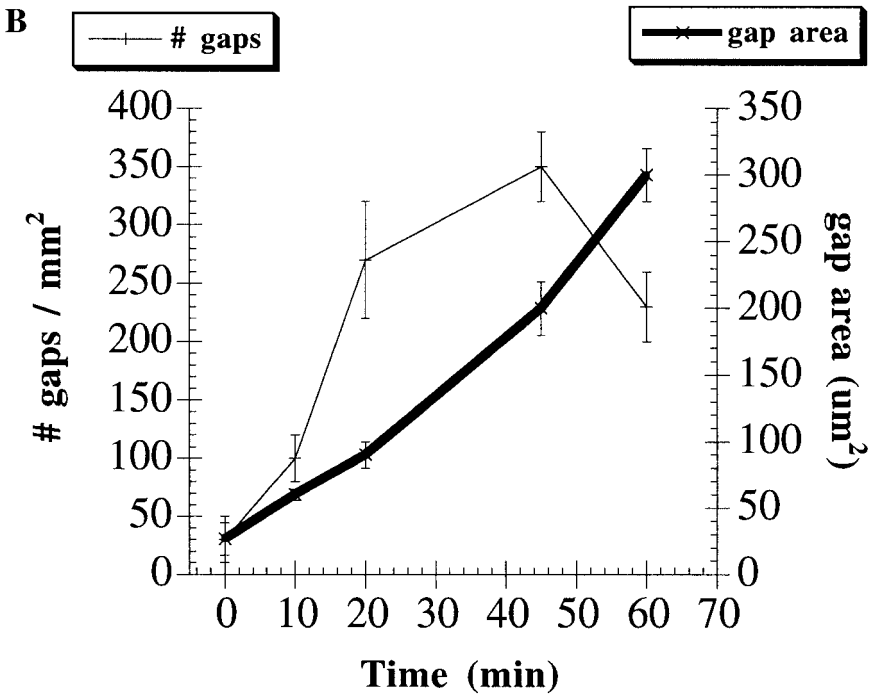

Fig. 10. Quantification of intercellular gap formation in the presence of a cell permeable peptide corresponding to a site on cofilin that binds PIP_2 (PIP_2 peptide). Thin line depicts no. of gaps/mm^2. Heavy line depicts average gap area (μm^2). **A:** Cells pretreated with PIP_2 peptide (10 μM) for 30 min prior to H_2O_2 (100 μM) for 1–30 min. **B:** Cells pretreated with control peptide (10 μM) for 30 min prior to H_2O_2 (100 μM) for 1–30 min. Pretreated cells are compared with H_2O_2-treated cells: $^*P < 0.05$. There is no significant difference between the control peptide-pretreated cells and H_2O_2 (alone)-treated cells. Error bars = means ±SD (n = 3 for each group).

location, which suggests that EC filamin distribution is also dependent on cellular PIP_2 levels.

ACKNOWLEDGMENTS

The authors thank Qin Wang and Nancy Chung-Welch for useful discussions and careful reading of this manuscript.

REFERENCES

Amsterdam A, Dantes A, Liscovitch M (1994): Role of phospholipase D and phosphatidic acid in mediating gonodotropin-releasing hormone-induced inhibition of preantral granulosa cell differentiation. Endocrinology 135:1205–1211.

Burstein S, Budrow J, Debatis M, Hunter S, Subramanian A (1994): Phospholipase participation in cannabinoid-induced release of free arachidonic acid. Biochem Pharmacol 48:1253–1264.

Carney D, Scott D, Gordon E, LaBelle E (1985): Phosphoinositides in mitogenesis: neomycin inhibits thrombin-stimulated phosphoinositide turnover and initiation of cell proliferation. Cell 42:479–488.

Cross M, Roberts S, Ridley A, Hodgkin M, Stewart A, Claesson-Welsh L, Wakelam M (1996): Stimulation of actin stress fibre formation mediated by activation of phospholipase D. Curr Biol 6:588–597.

Dejana E, Cordada M, Lampugnani M (1995): Endothelial cell-to-cell junctions. FASEB J 9:910–918.

Furuhashi K, Inagaki M, Hatano S, Fukami K, Takenawa T (1992): Inositol phospholipid-induced suppression of F-actin gelating activity of smooth muscle filamin. Biochem Biophys Res Commun 184:1261–1265.

Gabev E, Kasianowicz J, Abbott T, McLaughlin S (1989): Binding of neomycin to phosphatidylinositol 4,5-bisphosphate (PIP_2). Biochim Biophys Acta 979:105–112.

Goldman G, Welbourn R, Alexander S, Wiles M, Valeri C, Shepro D, Hechtman H (1991): Modulation of pulmonary permeability in vivo with agents that affect the cytoskeleton. Surgery 109:533–538.

Hastie L, Patton W, Hechtman H, Shepro D (1997a): Filamin redistribution in an endothelial cell reoxygenation injury model. Free Radic Biol Med 22:655–666.

Hastie L, Patton W, Hechtman H, Shepro D (1997b): H_2O_2-induced filamin redistribution in endothelial cells is modulated by the cyclic AMP dependent protein kinase pathway. J Cell Physiol 172:373–381.

Janmey P (1994): Phosphoinositides and calcium as regulators of cellular actin assembly and disassembly. Annu Rev Physiol 56:169–191.

Johnson A, Phillips P, Hocking D, Tsan M, Ferro T (1989): Protein kinase inhibitor prevents pulmonary edema in response to H_2O_2. Am J Physiol 256:H1012–H1022.

Kiss Z, Anderson W (1994): Hydrogen peroxide regulates phospholipase D mediated hydrolysis of phosphatidylethanolamine and phosphatidylcholine by different mechanisms in NIH 3T3 fibroblasts. Arch Biochem Biophys 311:430–436.

Liu SM, Sundqvist T (1995): Effects of hydrogen peroxide and phorbol myristate acetate on endothelial transport and F-actin distribution. Exp Cell Res 217:1–7.

Lum H, Malik A (1994): Regulation of vascular endothelial barrier function. Am J Physiol 267:L223–L241.

Marcoz P, Nemoz A, Prigent A, Lafgarde M (1993): Phosphatidic acid stimulates the rolipram-sensitive cyclic nucleotide phosphodiesterase from rat thymocytes. Biochim Biophys Acta 1176:129–136.

Moritz A, DeGraan P, Gispen W, Wirtz K (1992): Phosphatidic acid is a specific activator of phosphatidylinositol-4-phosphate kinase. J Biol Chem 267:7207–7210.

Murayama T and Ui M (1987): Phosphatidic acid may stimulate membrane receptors mediating adenylate cyclase inhibition and phospholipid breakdown in 3T3 fibroblasts. J Biol Chem 262:5522–5529.

Naccache P, Caon A, Gilbert C, Gaudry M, Roberge C, Poubelle P, Bourgoin S (1993): Inhibition of tyrosine phosphorylation by wortmannin in human neutrophils. Dissociation from its inhibitory effects on phospholipase D. Lab Invest 69:19–23.

Natarajan V, Taher MM, Roehm B, Parinandi NL, Schmid HHO, Kiss Z, Garcia JGN (1993): Activation of endothelial cell phospholipase D by hydrogen peroxide and fatty acid hydroperoxide. J Biol Chem 268:930–937.

Natarajan V, Vepa S, Verma R, Scribner W (1996): Role of tyrosine phosphorylation in H_2O_2-induced activation of endothelial cell phospholipase D. Am J Physiol 271:L400–L408.

Patton W, Alexander JS, Dodge AB, Patton RJ, Hechtman H, Shepro D (1991): Mercury arc photolysis: a method for examining second messenger regulation of endothelial cell monolayer integrity. Anal Biochem 196:31–38.

Ramsby ML, Makowski GS, Khairallah EA (1994): Differential detergent fractionation of isolated hepatocytes: biochemical, immunochemical and two-dimensional gel electrophoresis characterization of cytoskeletal and noncytoskeletal compartments. Electrophoresis 15:265–277.

Shasby DM, Yorek M, Shasby SS (1988): Exogenous oxidants initiate hydrolysis of endothelial cell inositol phospholipids. Blood 72:491–499.

Shepro D, Rosenthal M, Batbouta J, Roblee LS, Belamarich FA (1974): The cultivation of aortic endothelium. Anat Rec 78:52.

Spragg RG, Hinshaw DB, Hyslop PA, Schraufstatter IU, Cochrane CG (1985): Alterations in adenosine triphosphate and energy charge in cultured endothelial and $P388D_1$ cells after oxidant injury. J Clin Invest 76:1471–1476.

Towbin H, Staehlin T, Gordon J (1979): Electrophoretic transfer of protein from polyacrylamide cells to nitrocellulose sheets: Procedures and some applications. Proc Natl Acad Sci USA 76:4350–4354.

Tsai M, Yu C, Stacey D (1989): The effect of GTPase activating protein upon ras is inhibited by mitogenically responsive lipids. Science 243:522–526.

van Corven EJ, Groenink A, Jalink K, Eicholtz T, Moolenaar WH (1989): Lysophosphatidate-induced cell proliferation: Identification and dissection of signaling pathways mediated by G proteins. Cell 59:45–54.

Varani J, Phan SH, Gibbs DF, Ryan US, Ward PA (1990): H_2O_2-mediated cytotoxicity of rat pulmonary endothelial cells. Changes in adenosine triphosphate and purine products and effects of preventive interventions. Lab Invest 63:683.

Wang Q, Patton W, Chiang E, Hechtman H, Shepro D (1996): Filamin translocation is an early inflammatory response to bradykinin: Regulation by calcium, protein kinases and protein phosphatases. J Cell Biochem 62:383–396.

Welbourn R, Goldman G, Paterson I, Valeri C, Shepro D, Hechtman H (1991): Pathophysiology of ischaemia reperfusion injury: Central role of the neutrophil. Br J Surg 78:651–655.

Wiles M, Hechtman HB, Morel NML, Shepro D (1993): Hypoxia/reoxygenation induced injury of cultured pulmonary microvessel endothelial cells. J Leuk Biol 53:490–497.

Yeh Y, Herenyiova M, Weber G (1995): Quercetin: synergistic action with carboxyamidotriazole in human breast carcinoma cells. Life Sci 57:1285–1292.

Yonezawa N, Homma Y, Yahara I, Sakai H, Nishida E (1991): A short sequence responsible for both phosphoinositide binding and actin binding activities of cofilin. J Biol Chem 266:17218–17221.